Mass-independent Isotope Anomalies of Titanium in Carbonaceous Chondrites:

Implications for Isotopic Heterogeneity in the Early Solar System

by

Nicole Danielle Phelan

A Thesis Presented in Partial Fulfillment
of the Requirements for the Degree
Master of Science

Approved June 2023 by the
Graduate Supervisory Committee:

Meenakshi Wadhwa, Chair
Patrick Young
Larry R. Nittler

ARIZONA STATE UNIVERSITY

August 2023

ABSTRACT

The isotopic compositions of meteorites provide valuable insights into the earliest history of the Solar System and, in some cases, provide constraints on presolar components that contributed to the solar nebula. In the past decade or so, mass-independent isotope anomalies in titanium have become particularly important geochemical tracers to study the distinct isotopic reservoirs in the early Solar System. In particular, mass-independent anomalies in the most neutron-rich isotope of titanium (^{50}Ti) have been used to distinguish between carbonaceous chondritic (CC) and non-carbonaceous chondritic (NC) materials. These two groupings likely represent distinct isotopic reservoirs in the inner (NC) and outer (CC) Solar System. However, while the titanium isotope compositions of CC and NC materials are distinct, each group's full range of compositional variability is poorly characterized. For example, only one CK carbonaceous chondrite group member has been analyzed thus far for its bulk Ti isotope composition.

This work aims to characterize better the range of mass-independent Ti isotope compositions within and among the carbonaceous chondrites, which has implications for the degree and potential sources of Ti isotope heterogeneity in the early Solar System. Methods utilized in this study include column chromatography to purify Ti and high-precision multi-collector inductively coupled plasma mass spectrometry for measuring Ti isotope compositions. The Ti isotope compositions of bulk samples of nine carbonaceous chondrites are reported here. In addition, the bulk fractions of the meteorites used in this study were taken from homogenized powders of relatively large (~200 mg each) samples.

i

This was done to assess whether variability in mass-independent Ti isotope compositions previously reported within some meteorites could be a sampling artifact.

Results from this work show that the various CM2 chondrites and ungrouped carbonaceous chondrites have ε^{50}Ti values that are similar, suggesting that the Ti in these samples was likely sourced from a common isotopic reservoir. On the other hand, the ε^{50}Ti values reported for CI1 and CH/CBb bulk samples suggest that the parent bodies of these carbonaceous chondrite groups were formed in isotopic reservoir(s) distinct from that of the other CC groups in the early Solar System.

DEDICATION

This thesis is dedicated to my parents, to whom I owe everything.

ACKNOWLEDGMENTS

TABLE OF CONTENTS

LIST OF TABLES

LIST OF FIGURES

1. INTRODUCTION

Meteorites offer an opportunity to study physical samples from various Solar System bodies and provide evidence that the Solar System is comprised of a mixture of components sourced from a variety of stellar environments pre-dating the Sun. Meteorites are broadly separated into two groups based on whether the parent bodies from which they originated have undergone melting ("differentiated") or not ("undifferentiated"). This study focuses on undifferentiated samples called chondrites. By studying the isotope compositions of these chondrite samples and their components, researchers can address questions related to the history of the Solar System, such as the nucleosynthetic sources, accretional environments, and processing events of the parent bodies from which these meteorites originated. In particular, mass-independent isotopic anomalies in chondrite materials are used to infer the temporal and spatial extent of mixing processes in the protoplanetary disk (e.g., Dauphas and Schauble, 2016).

1.1. Carbonaceous Chondrites and their Components

As chondrites are undifferentiated material, they and their components are considered to represent some of the earliest conditions of the Solar System. Chondrites are varied in mineralogy but are generally ultramafic in their bulk compositions (Krot et al., 2014). Chondrites host a variety of components, including chondrules, calcium-aluminum inclusions (CAIs), and matrix material. Chondrites are typically grouped into four major classes: Carbonaceous, Ordinary, Enstatite, and "Other." These chondrite classes are then further divided into 'clans' and then divided once more into smaller 'groups' based on geochemical and mineralogical similarities between samples (Figure 1). Furthermore, an

1

indication of a sample's petrologic type, or the amount of parent body thermal processing, is often noted as a number at the end of the classification acronym (i.e., 1-6).

The term '*carbonaceous*' is considered a planetary science misnomer as not all carbonaceous chondrites are enriched in carbon relative to non-carbonaceous materials (only CI, CM, and CR groups are (Krot et al., 2014)). The bulk compositions of the CI group most closely match the solar photosphere elemental abundance, excluding some highly volatile elements (e.g., hydrogen, carbon, nitrogen), and are therefore used as a reference composition for most Solar System materials (Barrat et al., 2012). Other carbonaceous chondrite groups are often categorized as such based on their refractory element abundance (similar to or above those of CI chondrites) and their oxygen isotope compositions (Krot et al., 2014). In the past decade or so, isotopic anomalies in elements, such as Ti (as will be discussed further in section 1.3), have been used to separate carbonaceous chondrites (CC) from non-carbonaceous chondrites (NC) in a broader sense.
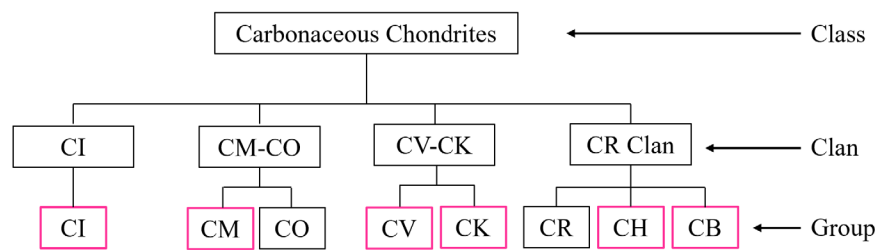
Figure 1. Diagram of carbonaceous chondrite classifications, showing the primary carbonaceous class, clans, and groups. Groups from which samples in the study were derived are indicated in a pink box. Diagram after Weisberg et al. (2006).

1.2. Presolar Grains in Early Solar System Materials

The protoplanetary disk has historically been considered a high-temperature, well-homogenized environment from which the Solar System eventually formed (Urey 1952; Bermingham 2020). Observations that eventually led to a new concept of a cooler and heterogenous disk (e.g., Clayton 1982) included the discovery of isotopic variations of xenon in meteorites (e.g., Reynolds and Turner 1964) and isotopic variations for neon (Ne) and xenon (Xe) in silicon carbide (SiC) grains (Bernatowicz et al., 1987). With this concept in mind and the constantly improving mass spectrometry instrumentation, isotopic measurements of meteorites began to reveal variations in their bulk samples and components that could not be explained by mass-dependent processes, radioactive decay, or space weathering effects (Bemingham et al., 2020). These so-named *nucleosynthetic isotope anomalies* are thought to be remnant signatures of a heterogeneous distribution of presolar grains in the protoplanetary disk (Qin and Carlson 2016).

Presolar grains are known to be anomalous in all measured isotope ratios, whereas other chondrite materials, such as CAIs, are only anomalous in some isotopic ratios (Zinner 2014). Furthermore, they can come in various oxide or silicate phases; even carbides and metal phases have been found as sub-grains inside some silicon-carbide presolar grains. Of all the presolar grain types, silicon carbide (SiC) has been studied the most. SiC grains are divided into subgroups based on isotopic data for carbon, nitrogen, and silicon (Hoppe and Ott, 1997); the groupings are as follows: mainstream, AB, C, X, Y, Z, and nova grains. Mainstream grains are the most abundant of these subtypes. They are considered to be sourced from carbon stars during the asymptotic giant branch (AGB)

phase of evolution due to their closely matching $^{12}C/^{13}C$ ratios (Zinner, 2014; Lambert et al., 1986). Of the remaining SiC sub-groups, AB, C, and X grains have been proposed as potentially being sourced from supernovae (e.g., AB: Liu et al., 2017; C: Hoppe et al., 2012; X: Amari et al., 1992).

For this study, it is crucial to understand the proposed sources for the most neutron-rich Ti isotope (^{50}Ti), as this is the isotope that is most notably used to distinguish between non-carbonaceous and carbonaceous chondritic materials (Figure 2). ^{50}Ti requires extremely neutron-rich conditions to form and is therefore thought to be sourced from type SNIa or electron capture supernovae as well as minor amounts which may have been formed during the slow neutron capture (s-process) in the He burning shells of massive and AGB stars (e.g., Clayton 2003; Torrano et al., 2023; Nittler et al., 2018). Other presolar grain types, such as silicates and oxides, are not as well studied due to their small sizes (submicron size (Zinner, 2014)) and susceptibility to the dissolution processes typically used to separate SiC presolar grains from a sample matrix. Despite this, it is essential to consider these presolar grains as another source of anomalous isotope signatures seen in chondrite bulk samples.

1.3. Ti Isotope Anomalies in Bulk Samples of CC and Their Components

Titanium has five naturally occurring stable isotopes (^{46}Ti, ^{47}Ti, ^{48}Ti, ^{49}Ti, and ^{50}Ti). Bulk sample chondrite isotope anomalies in the most neutron-rich stable isotope of titanium (^{50}Ti) became of interest when it was found that they could be used to distinguish between carbonaceous chondritic (CC) and non-carbonaceous chondritic (NC) materials (e.g., Figure 2 of Trinquier et al., 2009). These two groupings likely

4

represent distinct isotopic reservoirs in the inner (NC) and outer (CC) Solar Systems that

are suggested to result from the early formation of Jupiter (Kruijer et al., 2017). Of the

stable Ti isotopes, ^{46}Ti and ^{50}Ti are the only isotopes to display a correlated anomaly.

This was determined because, apart from CAIs and AOAs, bulk meteorites have a

^{48}Ti/^{47}Ti ratio that is terrestrial in composition when the ^{49}Ti/^{47}Ti ratio is used in

instrument mass fractionation corrections; if a different ratio pair is used (e.g., ^{49}Ti/^{48}Ti or

^{48}Ti/^{47}Ti) for this correction, the correlated ^{46}Ti and ^{50}Ti anomalies would still be present

(Trinquier et al., 2009). Measuring the bulk sample compositions of ε^{50}Ti (ε – parts per

ten thousand deviations from the standard) provides insight into the chondrite parent

body's history and its relation to other parent bodies, whereas measuring the various

components of a chondrite (e.g., calcium-aluminum-rich inclusions (CAIs)) provides

information on the region of the solar nebula in which the material condensed.

While the bulk sample titanium isotope compositions of CC and NC materials are

distinct, the full range of compositional variability within each group is unclear. Till now,

only a few members of each carbonaceous chondrite (CC) group have been analyzed thus

far. For instance, the ε^{50}Ti value for CK chondrites is based on two separate

measurements of the Karoonda (CK4) meteorite (Trinquier et al., 2009; Zhang et al.,

2012). Furthermore, the Ti isotope variability in samples measured in multiple studies

(e.g., Murchison (CM2) data reported in Trinquier et al., 2009; Torrano et al., 2021, and

this study) could indicate inhomogeneity between separate powdered aliquots of the same

sample. To address this, larger bulk fragments were powdered and homogenized for this

study. Considering the above, this work aims to better characterize the variability of Ti

isotope compositions within and among the carbonaceous chondrites, which has

implications for the degree and potential sources of Ti isotope heterogeneity in the early

Solar System. This work reports new measurements of the Ti isotope compositions using

analytical methods that allow precise measurements of Ti isotope compositions for the

bulk samples of several carbonaceous chondrites.
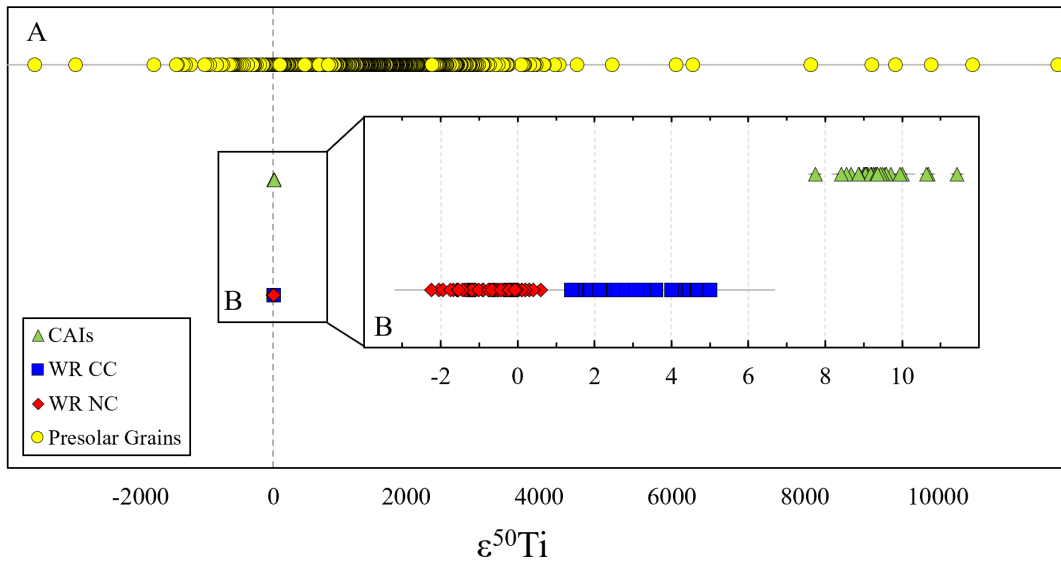
Figure 2. ^{50}Ti/^{47}Ti values (expressed in ε units) in presolar grains, CAIs, and "whole rock" (WR) samples of CC- and NC-type meteorites (both of which include various chondrite and achondrite types). Error bars are shown in gray. Figure modified from Bermingham et al. (2020) and Torrano et al. (2019). Presolar grain data from Hynes and Gyngard (2009) and references therein. CAI data from Torrano et al. (2019) and Trinquier et al. (2009). Whole rock data from Leya et al. (2007), Sanborn et al. (2019), Torrano et al. (2021), Trinquier et al. (2009), Williams et al. (2020), Zhang et al. (2012), and Metzler et al. (2021).

2. SAMPLES

A suite of nine carbonaceous chondrites was examined in this study (Table 1). Some

samples have been measured previously (e.g., Trinquier et al., 2009; Torrano et al.,

2021), while others have not.

Table 1. List of the samples analyzed in this study.

Sample Name	Sample ID	Classification	Fall/Find	Ti Isotopes Measured Previously?	Mass Powdered (mg)	Mass Dissolved (mg)	Ti (ppb)[*]
Orgueil	ASU 2225	CI1	Fall	Yes[1,2]	209.28	51.98	1562
Murchison	ASU 828	CM2	Fall	Yes[1,3]	203.38	28.14	1153
Jbilet Winselwan	ASU 1810-3	CM2	Find	No	235.30	55.33	2278
Maralinga	ASU 1352.6	CK4$_{anomalous}$	Find	No	197.38	29.48	1645
Isheyevo	ASU 1580	CH/CB$_b$	Find	No	-	199.6	2821
Tarda	ASU 2149-1	C2$_{ungrouped}$	Fall	No	209.59	37.66	1324
Tagish Lake	ASU 1767-9	C2$_{ungrouped}$	Fall	Yes[1]	205.01	48.21	2014
Sutter's Mill	ASU 1684	C	Fall	No	197.90	38.52	1607

*Concentration measurements are from this study and were performed using an iCAP-Q ICP-MS (uncertainty of elemental concentration values is ± 10%). Previously performed mass-independent Ti isotope measurement sources: [1]Trinquier et al., (2009), [2]Zhang et al. (2012), [3]Torrano et al. (2021).

2.1. CI Samples

Orgueil (CI1) was the only CI chondrite measured in this study. While most carbonaceous chondrites are abundant in chondrules, Orgueil's mineralogy is dominated by a dark, fine-grained matrix (Tomeoka & Buseck, 1988). The widely studied composition of Orgueil's matrix (e.g., Phan et al., 2022 and references therein) has found that the matrix is dominated by phyllosilicates of small grain size (<1 um) with some larger aggregates (Tomeoka & Buseck, 1988) while the second most abundant phase has been interpreted as a hydrated sulfate (Phan et al., 2022).

2.2. CM Samples

The two CM samples measured in this study were Murchison and Jbilet Winselwan. Jbilet Winselwan is heavily brecciated with clasts ranging from petrologic type 2.0 to 2.7 (Van Kooten et al., 2018 and references therein). It has been suggested that Jbilet Winselwan is representative of a C-type asteroid regolith with lithologies that show signs of impact heating (Kooten et al., 2018; Zolensky et al., 2016). A recent study found two

hibonite or spinel crystal inclusions in Jbilet Winselwan with nucleosynthetic Ti isotope signatures far different from the population or regular CAIs (Render et al., 2019). The study suggested that these aggregates found in Jbilet Winselwan may represent earlier refractory material condensed before other CAIs (Render et al., 2019). Murchison is classified as a CM2 chondrite and has been studied extensively. It consists of a regolith breccia (Krot et al., 2014) and is often used in studies of presolar silicon-carbide (SiC) grains (e.g., Nguyen et al., 2018; Hoppe et al., 2000).

2.3. CK Samples

Maralinga was the one CK chondrite sample to be measured in this study. It is a metamorphosed carbonaceous chondrite (CK4) composed of a fine-grained matrix and millimeter-sized chondrules. Maralinga is currently sub-grouped as an anomalous CK chondrite due to its large amount of chondrules (nearly 50 % by volume) and high abundance of refractory inclusions compared to other CK samples (Keller et al., 1992). A previous study on one of Maralinga's CAIs revealed a complex history that involved the formation and breakdown of precursor phases in redox conditions ranging from highly reducing to strongly oxidizing (Kurat et al., 2002). Before this study, the only CK chondrite with measured bulk sample Ti isotope compositions was the CK4 sample, Karoonda (Trinquier et al., 2009; Zhang et al., 2012).

2.4. CH/CB Samples

Isheyevo, a CH/CB$_b$ chondrite, is a unique meteorite sample as it contains characteristics from both the CH and CB$_b$ groupings, hence the CH/CB$_b$ classification. Isheyevo does not contain inter-chondrule matrix material; the only fine-grained material

in the sample is described as chondritic lithic clasts of foreign origin (Bonal et al., 2010). The metal-rich lithologies are similar to the CB group. In contrast, the metal-poor lithologies are most similar to CH chondrites (Ivanova et al., 2008) Isheyevo is comprised of 50% to 70% volume of Fe-Ni metal (Russell et al., 2005). Due to its high metal content, this sample was processed differently than other CC samples (as described in section 3.1). Like CH chondrites, the CAI types most often found in the Isheyevo sample are hibonite, melilite- and grossite-rich (Ivanova et al., 2008).

2.5. Ungrouped Samples

Sutter's Mill is currently classified as a C-ungrouped chondrite in the Meteoritical Society's Meteoritical Bulletin Database. Many studies have called for the sample reclassification to a "CM" chondrite due to its mineralogical similarities to the CM group (Zolensky et al., 2014). Sutter's Mill consists of regolith breccia with CM1-CM2 lithologies, including chondrules and CAIs, which have undergone partial to complete aqueous alteration (Zolensky et al., 2014).

Tagish Lake is considered a C2-ungrouped chondrite. The classification of C2 was determined due to the pervasive but incomplete aqueous alteration and high carbon and water content (Zolensky et al., 2002). Significant isotopic variations (e.g., in N) in the Tagish Lake sample have been measured, which have been argued to indicate high presolar grain content (Brown et al., 2000). The bulk chemistry, the common presence of hydrous phyllosilicates, and its unique oxygen isotope content make Tagish Lake different from the CI1 and CM2 samples measured, leaving its classification to remain a C2-ungrouped chondrite (Zolensky et al., 2002).

9

Tarda, like Tagish Lake, is currently classified as a C2-ungrouped chondrite. A recent study showed that Tarda and Tagish Lake share similarities (e.g., O-isotope compositions and D-enrichment), likely linking these samples in a shared formational environment (Marrocchi et al., 2021). Tarda, like Tagish Lake, also shares an abundant fine-grained matrix with a lower abundance of chondrules and isolated olivine grains (Marrocchi et al., 2021). Tarda and Tagish Lake are now suggested to be sourced from a D-type asteroid accreted in the outer Solar System near Saturn (Marrocchi et al., 2021).

3. ANALYTICAL METHODS

All sample preparation and chemistry occurred at the Isotope Cosmochemistry and Geochronology Laboratory (ICGL) at Arizona State University. Robust methods for Ti element purification and isotopic analysis have been developed and used at the ICGL over several years (Torrano et al., 2019).

3.1. Sample Preparation and Digestion

Clean interior fragments of all the samples were obtained from the ASU Buseck Center for Meteorite Studies. All samples, excluding Isheyevo, were crushed and powdered using a clean agate mortar and pestle in the ICGL (Figure 3). These samples were treated with concentrated HCl on a hotplate for ~12 hours. Once cooled, most of the liquidus was removed and dried in a separate Teflon beaker. The remaining liquid and residue were dried and then treated with a 3:1 ratio of concentrated HF and HNO_3 on a hotplate overnight. The liquid from this treatment was again removed and dried in a separate Teflon jar. Any remaining liquidus and solidus from this second treatment were dried and then loaded into Parr high-pressure digestion vessels in a 3:1 ratio of

concentrated HF and HNO_3. After complete digestion using the Parrs, all sample aliquots (i.e., HCl, HF, and HNO_3 liquidus cut previously removed) were recombined and dried down.
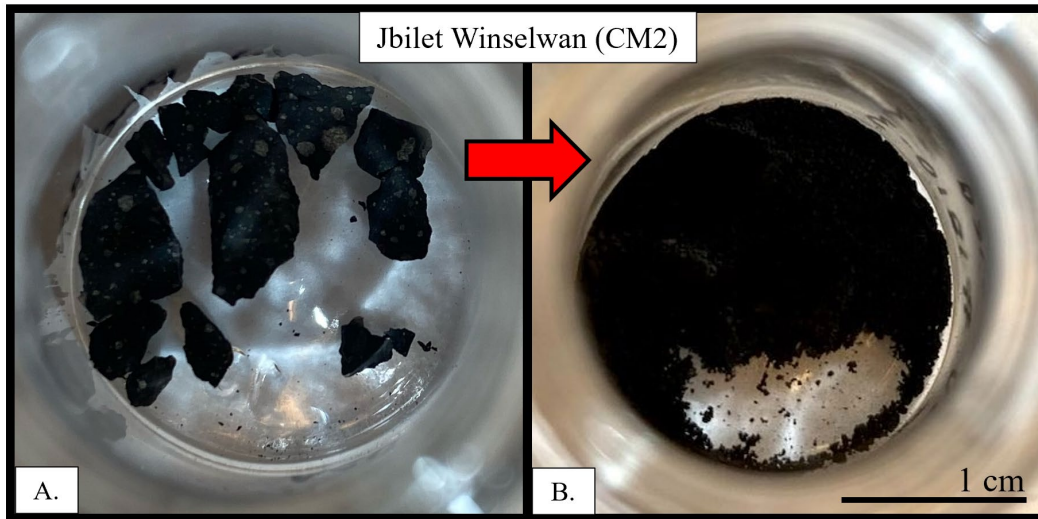
Figure 3. The Jbilet Winselwan (CM2) fragment prior to being powdered (A.) versus after powdering (B.) in the ICGL.

Due to its high metal content, the Isheyevo sample was not crushed. Instead, the sample fragment was first cleaned in 18.2 MΩ Milli-Q water (MQ H_2O) and then digested using concentrated HCl on a hotplate. The liquidus from the HCl treatment step was removed and dried in a separate Teflon beaker. This HCl treatment was repeated five times until most of the metal content had been brought into solution. The remaining sample residue was then treated with a 3:1 ratio of concentrated HF and HNO_3 on a hotplate. Again, the liquidus from this treatment was removed and dried in a separate Teflon beaker. Any remaining wet residue from this second treatment was dried and then loaded into Parrs in a 3:1 ratio of concentrated HF and HNO_3. After complete digestion

using the Parrs, all the separated fractions (i.e., HCl, HF, and HNO_3 liquidus cuts previously removed) were recombined and dried down.

Following complete digestion, the sample was brought into solution in 10 mL of 12 M HNO_3. An aliquot of 50 uL for each solution was measured for elemental concentrations using the iCAP-Q quadrupole ICP-MS in the Metals, Environmental, and Terrestrial Analytical Laboratory (METAL) at ASU.

3.2. Titanium Purification Chemistry

Ion exchange column chromatography using Eichron TODGA and AG1-X8 resins was performed to obtain pure titanium from a small aliquot (between 1.5 to 3.0 mL) of digested samples, according to methods described in Torrano et al. (2019) and Torrano et al. (2021). The detailed protocol used in this study is outlined in Table 2.

Table 2. Titanium Purification Method (adapted from Torrano et al., 2019)

Column 1 – TODGA 2 mL Cartridge (50-100 mesh)

Step	Reagent	Volume (mL)
Resin Cleaning	MQ H_2O	4
Resin Conditioning	12 M HNO_3	15
Load Sample	12 M HNO_3	10
Elute Matrix	12 M HNO_3	10
Elute Ti and Fe	6 M HNO_3	10
Elute Excess Fe	3 M HNO_3	10
Elute Zr and Hf	3 M HNO_3 – 0.3 M HF	20
Elute REE	0.2 M HF	20
Post-Chemistry Resin Cleaning	0.5 M HCl	10
Post-Chemistry Resin Cleaning	MQ H_2O	10
Post-Chemistry Resin Cleaning	Dry Resin in Cartridge	

Column 2 – AG1-X8 1 mL (200-400 mesh)

Step	Reagent	Volume (mL)
Resin Cleaning	3 M HNO_3	10
Resin Cleaning	MQ H_2O	18
Resin Cleaning	6 M HCl	12
Resin Conditioning	6 M HCl	5
Load Sample	6 M HCl	1

Elute Ti	6 M HCl	4
Elute Fe	0.5 M HCl	8
Elute Zn	3.0 M HNO_3	6

The first column procedure used a 2 mL Eichrom 50-100 mesh DGA resin cartridge attached to the Luer lock of a 30 mL BD Slip-Tip syringe barrel. The column was pressurized using a manifold that supplied clean, dry, ultra-high-purity nitrogen. The pressure was maintained to get ~1 mL of reagent passed through the column per minute. For the first column, 10 mL of 6 M HNO_3 was used to co-elute Ti and Fe from the resin cartridge; a secondary Fe separation column procedure (Torrano et al., 2019) was then used to separate Ti and Fe.

An aliquot corresponding to ~5 ug of Ti in 10 mL of 12 M HNO_3 (see section 3.1) was chemically processed using the abovementioned methods. Column chemistry was performed in batches of 2-3 samples with a BCR-2 terrestrial standard, Allende (CV3) chondrite standard, and a procedural blank. Purified Ti sample cuts were measured on the METAL iCAP-Q quadrupole ICP-MS to check the concentration of potential isobaric interferences, Ti yields, and the total procedural blanks. All sample ratios of Ca/Ti, V/Ti, and Cr/Ti (which can cause potential isobaric interferences for Ti isotopic measurements) are well below the thresholds established by Zhang et al. (2011). Ti yields from these procedures regularly exceeded 95%, and the averaged total procedural blank for the chemical processing was <8 ng of Ti.

3.3. Titanium Isotope Analysis

Titanium isotopic measurements were performed using a Thermo Neptune XT multi-collector inductively coupled plasma mass spectrometer (MC-ICPMS) at the ICGL.

Before analysis, the purified Ti samples were diluted to a concentration of ~600 ppb in 3% HNO_3. The MC-ICPMS was run in high-resolution mode (where mass resolving power is > 8000) using an H-skimmer cone and a Jet sample cone. Samples were introduced using an Aridus3 or Elemental Scientific Apex-Ω desolvating nebulizer attached to a self-aspirating PFA nebulizer, with a 50 μL/min uptake rate. Sample uptake time was set between 70 s and 80 s, with a wash time between the successive sample and standard measurements set between 120 s and 130 s. Repeat measurements for the samples, standards, and blanks consisted of 30 cycles with an 8 s integration time per cycle. The average beam intensity of >20 V for ^{48}Ti was obtained. All the Faraday cups were attached with a 10^{11} Ω resistor amplifier. Two cup configurations were used to collect Ti isotope data. The first configuration measured the intensities of ^{44}Ca, ^{46}Ti, ^{47}Ti, ^{48}Ti and ^{49}Ti while the second cup configuration monitored ^{47}Ti, ^{49}Ti, ^{50}Ti, ^{51}V and ^{52}Cr. The ^{44}Ca, ^{51}V, and ^{52}Cr measured intensities were used as isobaric interference corrections on the ^{46}Ti, ^{48}Ti, and ^{50}Ti masses.

Data reduction, including corrections for the blanks, instrument mass fractionation, and interferences, were performed offline using Iolite (Paton et al., 2011). Ti compositions are reported relative to the NIST-3162a Ti standard solution, following corrections for instrumental mass bias and mass-dependent fractionation by sample-standard bracketing. Finally, internal normalization to ^{49}Ti/^{47}Ti (=0.749766, Niederer et al., 1981) is applied using the exponential mass fractionation law:

$$R = r[1 + \frac{\Delta m}{m}]^{\beta}$$

R represents the actual isotopic ratio, *r* is the measured Ti isotopic ratio, *Δm/m* is the

relative mass difference between the various Ti isotopes measured, and *β* symbolizes the

instrumental mass bias.

Final Ti isotope sample compositions are expressed in ε notation (i.e., parts per ten

thousand deviations from the NIST-3162a standard) as shown in the equation below:

$$\varepsilon^{i}Ti=[(^{i}Ti/^{47}Ti)_{sample}/(^{i}Ti/^{47}Ti)_{standard}-1]\times10^{4}$$

The ICGL's long-term external reproducibility for repeat analyses (n = 45) of the

synthetic (NIST-3162a and SPEX) and natural rock (BCR-2) standards throughout this

study is shown in Figure 4 (A, B, and C). The results of this study show that the methods

used to assess the mass-independent variations in Ti isotope ratios for the terrestrial

external standard BCR-2 are consistent with data reported in previous studies both

conducted outside of and at the ICGL (e.g., Torrano et al., 2019; Torrano et al., 2021;

Davis et al., 2018). All errors are reported as the larger of either the 2SD of all synthetic

and natural rock standards measured over the course of this study (n = 45) or the 2SE of

repeat analyses of an individual sample (typically six repeats of 30 cycles).
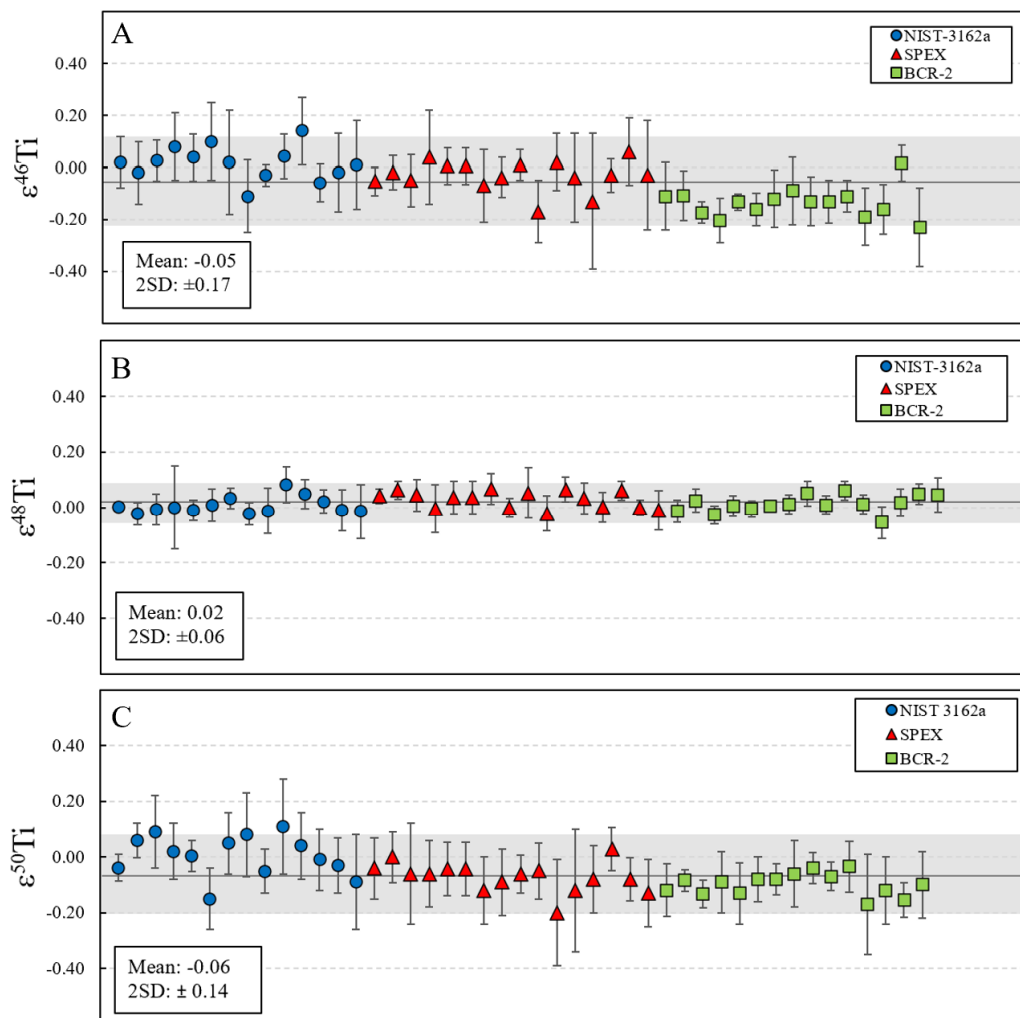
Figure 4. Synthetic (NIST-3162a and SPEX) and natural rock (BCR-2) standards were measured throughout this study for their ε^{46}Ti (A), ε^{48}Ti (B), and ε^{50}Ti (C) values. The error bars represent the 2SE of repeat measurements (typically 6) of an individual standard sample. The 'mean' and '2SD' indicated in each figure subplot are calculated using the measurements of all standards and represent the ICGL's external reproducibility for measurements taken throughout this study (n = 45).

4. RESULTS

4.1. Ti Isotope Measurements for Allende (CV3)

The ε^{50}Ti, ε^{48}Ti and ε^{46}Ti values for the Allende (CV3) chondrite fall within the

expected range based on data reported previously for this meteorite (e.g., Figure 5 of

16

Torrano et al., 2019). This study used two independently digested Allende solutions (Allende 1 & Allende 2). Both samples were digested from the Smithsonian Allende Reference Powder. While this powder is homogenized well, presolar grains could be incorporated into some sample aliquots, leading to variations in Ti isotopic measurements between sample aliquots, particularly for ε^{50}Ti values. It should also be noted that while the blanks measured in this study were low (<8 ng of Ti), even a minor amount of Ti contamination (i.e., pg amount) can affect a sample's ε^{50}Ti value as it is far more anomalous compared to an ε^{48}Ti value. This is likely a case for variations seen in the sample aliquots from this study.
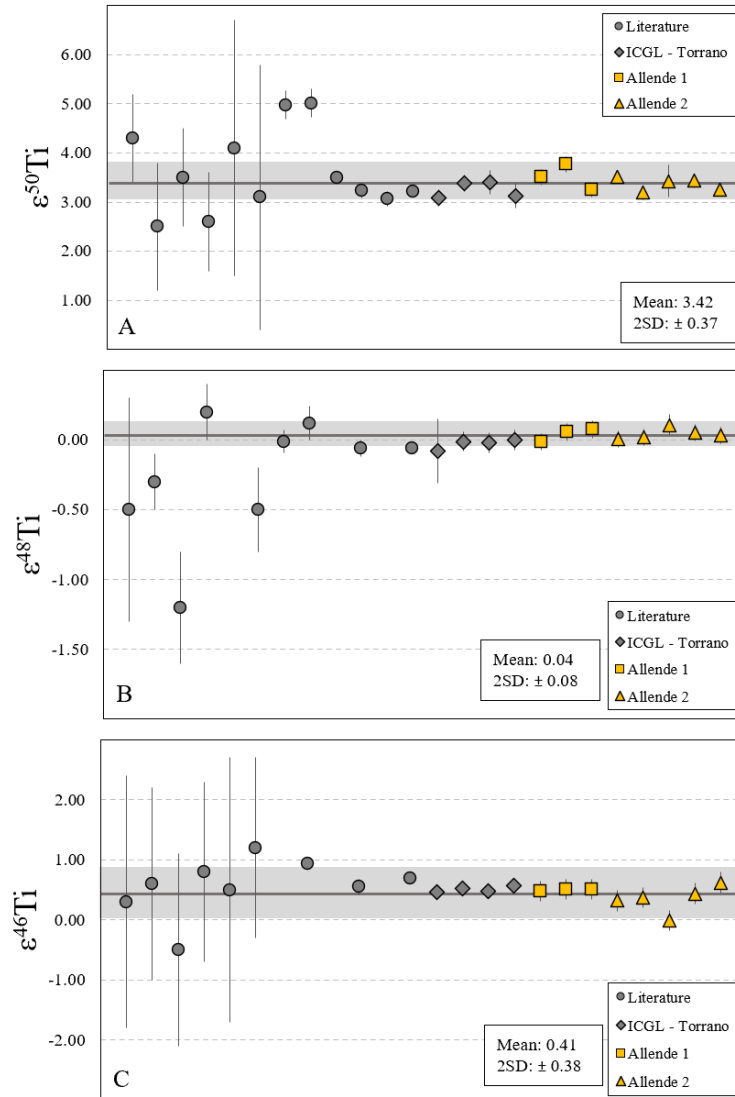
Figure 5. ε^{50}Ti (A), ε^{48}Ti (B), and ε^{46}Ti (C) values for Allende (CV3) from previous studies (grey circles & grey diamonds), as well as the Allende 1 (yellow squares) and Allende 2 (yellow triangles) solutions used in this study. Note that the ε^{48}Ti and ε^{46}Ti values were not reported for all samples in the literature data (shown as a blank space). All other points on plots A, B, and C align to indicate the different isotopic measurements from the same sample aliquot. The "Mean" (solid line) and "2SD" (grey rectangle) were calculated using the sample measurements from this study (Allende 1 and Allende 2). The error on each data point shown here is the larger of either the 2SE of repeat analyses of an individual sample or the 2SD based on repeat measurements of synthetic and natural rock standards used in this study (n = 45) (i.e., external reproducibility).

18

4.2. Mass Independent ε^{50}Ti Values of Sample Suite

ε^{50}Ti values for the carbonaceous chondrites measured in this study can be found in Table 3 and Figure 6A. Two ε^{50}Ti values for the Murchison (CM2) chondrite measured in this study (2.77 ± 0.16 and 2.63 ± 0.15) are the same within uncertainty. These are consistent with some previously reported data but are at the lower end of these values (Trinquier et al., 2009; Torrano et al., 2021). Previous studies have suggested that presolar grains may not significantly impact the ^{50}Ti signatures in CC materials (Trinquier et al., 2009). Nevertheless, the presence of presolar silicon-carbide (SiC) grains in Murchison (e.g., Huss et al., 2003; Davidson et al., 2014) could potentially explain the ε^{50}Ti variation observed in previous data. It could be argued that some of those variations could result from inhomogeneous distributions of such grains on the smaller sampling scales of those studies. Jbilet Winselwan, the other CM2 analyzed here, showed ε^{50}Ti $= 2.79 \pm 0.15$, which agrees well with that for Murchison and other previously measured CM2 meteorites (Torrano et al., 2021). This suggests that Jbilet Winselwan likely originated on the same or a similar parent body as Murchison and other CM2 meteorites.

Sutter's Mill is currently classified as a C meteorite, although it shares similarities to the CM chondrite group (Ruzicka et al., 2014). Its ε^{50}Ti value of 2.53 ± 0.15 agrees, within the errors, to values reported here for the Murchison and Jbilet Winselwan CM2 chondrites; as such, it likely originated from the same or similar isotopic reservoir.

Maralinga, a CK4-anomalous meteorite, has two ε^{50}Ti values of 2.56 ± 0.17 and 2.41 ± 0.16 reported here. These are resolvably lower than the values for Karoonda (CK4)

reported earlier by both Zhang et al. (2012) (3.26 ± 0.10) and Trinquier et al. (2009) (4.00 ± 0.19). CK chondrites host a more significant abundance of CAIs than other CC groups (Dunham et al., 2023); therefore, sample aliquots for CK chondrites need to be carefully selected to be representative of the bulk sample. In addition, CAIs often carry a higher anomalous nucleosynthetic Ti isotope signature relative to bulk chondrite samples (e.g., Trinquier et al., 2009; Torrano et al., 2019), so a heterogenous distribution of these materials in sample aliquots could contribute to differences in the reported values. The new data from this study expands the previously reported ε^{50}Ti variation in the CK group and demonstrates the need for further analyses of such CK samples.

Two ε^{50}Ti values are reported here for Orgueil, a CI1 chondrite. These values (1.87 ± 0.24 and 2.14 ± 0.15) agree well with values reported previously (Trinquier et al., 2009; Zhang et al., 2012; Williams et al., 2020). However, the CI1 values for ε^{50}Ti are distinctly lower than other CC groups, suggesting this group was sourced from a separate isotope reservoir than the other groups.

Isheyevo is classified as a CH/CB$_b$ chondrite (Russell et al., 2005). This sample is the first CH/CB sample to be measured for bulk Ti isotope compositions. The bulk ε^{50}Ti value for Isheyevo is 1.50 ± 0.15, which is lower than that of bulk CI1 chondrites and lower than the ε^{50}Ti values reported for CB$_a$ chondrules in Trinquier et al. (2009) (average value (n = 3) ~2.00 ± 0.20).

Tagish Lake and Tarda are classified as ungrouped C2 (C2$_{ung}$) carbonaceous chondrites. A recent study showed that these two samples shared numerous similarities and suggested that they may be originated on a D-type asteroid in an outer region of the

Solar System beyond Saturn (Yves et al., 2021). Tagish Lake has an ε^{50}Ti value of 3.06 ±

0.15. This value is slightly higher than previously reported (2.76 ± 0.26, Trinquier et al.,

2009) but still within error. Trinquier et al. (2009) used homogenized sample sizes of 10

to 100 mg, which is lower than what is used (200 mg) in this study; it is possible that a

heterogeneous distribution of materials could account for the slight variations seen

between these two studies. Tarda, while measured for Ti concentrations (Yves et al.,

2021) and other mass-independent nucleosynthetic isotope ratios (e.g., μ^{54}Fe – Hopp et

al., 2022), has not had Ti isotope compositions reported in the literature. The ε^{50}Ti value

for Tarda, 2.49 ± 0.15, is lower than the values for Tagish Lake. While these samples

may be sourced from a separate isotopic reservoir than other CC materials (e.g., CM), the

Ti isotope signatures alone do not suffice for this distinction to be made.

4.3. Mass Independent ε^{48}Ti Values of Sample Suite

The ε^{48}Ti values for the carbonaceous chondrites measured in this study can be found

in Table 3 and Figure 6B. The Tagish Lake ε^{48}Ti value reported in this study (-0.21 ±

0.07) is lower than that of Trinquier et al. (2009) (0.09 ± 0.18). The Murchison ε^{48}Ti

values reported here (0.07 ± 0.06 & 0.11 ± 0.07) are slightly higher than those of

previous studies (e.g., Torrano et al. 2021) but are the same within error. The two Orgueil

ε^{48}Ti values reported here (both values are 0.02 ± 0.06) agree well with those reported in

the literature (Trinquier et al., 2009). Isheyevo (CH/CB$_b$), Tagish Lake (C2$_{ung}$), and Jbilet

Winselwan (CM2) produced ε^{48}Ti values visibly lower than zero compared to the other

chondrite samples (Figure 6B). While there is some variation in the ε^{48}Ti values between

chondrite samples, the data points all cluster closely around the terrestrial value (0.01 ±

0.06 (Table 3)).

4.4. Mass Independent ε^{46}Ti Values of Sample Suite

The ε^{46}Ti values for the carbonaceous chondrites measured in this study can be found

in Table 3 and Figure 6C. All samples measured in this study (excluding one Allende

value (-0.01 ± 0.17)) show a positive ε^{46}Ti value. Similar to the ε^{48}Ti value, the Tagish

Lake (C2$_{ung}$) ε^{46}Ti value reported here (0.27 ± 0.17) is slightly lower than the value

reported in Trinquier et al. (2009) (0.50 ± 0.10). The Orgueil ε^{46}Ti values reported here

(0.22 ± 0.17 & 0.21 ± 0.17) are also slightly lower but just within error of the value

previously reported (0.38 ± 0.07; Trinquier et al., 2009). Murchison ε^{46}Ti values

measured in this study fall well within previously reported values from Trinquier et al.

(2009) and Torrano et al. (2021).

Table 3. Ti isotopic composition (ε^{50}Ti, ε^{48}Ti, and ε^{46}Ti) for samples measured in this study.

Sample	Classification	ε^{50}Ti	ε^{48}Ti	ε^{46}Ti	n
Orgueil	CI1	1.87 ± 0.24	0.02 ± 0.06	0.22 ± 0.17	6
		2.14 ± 0.14	0.02 ± 0.06	0.21 ± 0.17	5
Murchison	CM2	2.77 ± 0.12	0.07 ± 0.06	0.29 ± 0.17	4
		2.63 ± 0.16	0.11 ± 0.07	0.50 ± 0.17	6
Jbilet Winselwan	CM2	2.79 ± 0.14	-0.23 ± 0.06	0.09 ± 0.17	5
Maralinga	CK4$_{anomalous}$	2.56 ± 0.17	0.04 ± 0.07	0.34 ± 0.17	6
		2.41 ± 0.16	0.11 ± 0.08	0.19 ± 0.17	6
Isheyevo	CH/CB$_b$	1.50 ± 0.14	-0.21 ± 0.07	0.34 ± 0.17	6
Sutter's Mill	C	2.53 ± 0.14	0.14 ± 0.06	0.18 ± 0.17	7
Tagish Lake	C2$_{ungrouped}$	3.06 ± 0.14	-0.21 ± 0.07	0.27 ± 0.17	6
Tarda	C2$_{ungrouped}$	2.49 ± 0.14	0.00 ± 0.07	0.27 ± 0.17	6

Allende[1]	CV3	3.51 ± 0.16	-0.01 ± 0.06	0.48 ± 0.17	4
		3.77 ± 0.16	0.06 ± 0.06	0.51 ± 0.17	4
		3.25 ± 0.14	0.08 ± 0.06	0.51 ± 0.17	6
Allende[2]	CV3	3.51 ± 0.14	0.01 ± 0.06	0.32 ± 0.17	6
		3.19 ± 0.14	0.02 ± 0.06	0.37 ± 0.17	6
		3.43 ± 0.33	0.11± 0.07	-0.01 ± 0.17	6
		3.44 ± 0.14	0.05 ± 0.06	0.44 ± 0.17	6
		3.26 ± 0.14	0.03 ± 0.06	0.62 ± 0.17	6
Allende Average	*(m = 8)*	*3.42 ± 0.37*	*0.04 ± 0.08*	*0.41 ± 0.38*	
BCR – 2		-0.12 ± 0.14	-0.01 ± 0.06	-0.11 ± 0.17	6
		-0.08 ± 0.14	0.02 ± 0.06	-0.11 ± 0.17	6
		-0.13 ± 0.14	-0.03 ± 0.06	-0.17 ± 0.17	6
		-0.09 ± 0.14	0.01 ± 0.06	-0.20 ± 0.17	6
		-0.13 ± 0.14	-0.01 ± 0.06	-0.13 ± 0.17	6
		-0.08 ± 0.14	0.01 ± 0.06	-0.16 ± 0.17	6
		-0.08 ± 0.14	0.01 ± 0.06	-0.12 ± 0.17	6
		-0.06 ± 0.14	0.05 ± 0.06	-0.09 ± 0.17	6
		-0.04 ± 0.14	0.01 ± 0.06	-0.13 ± 0.17	6
		-0.07 ± 0.14	0.06 ± 0.06	-0.13 ± 0.17	6
		-0.04 ± 0.14	0.01 ± 0.06	-0.11 ± 0.17	8
		-0.17 ± 0.14	-0.06 ± 0.06	-0.19 ± 0.17	5
		-0.12 ± 0.14	0.02 ± 0.06	-0.16 ± 0.17	6
		-0.15 ± 0.14	0.05 ± 0.06	0.02 ± 0.17	6
		-0.10 ± 0.14	0.05 ± 0.06	-0.23 ± 0.17	6
BCR – 2 Average	*(m = 15)*	*-0.10 ± 0.08*	*0.01 ± 0.06*	*-0.14 ± 0.11*	

n is the number of repeat analyses on an individual sample. m is the number of samples used to calculate the Allende and BCR-2 average values and 2SD (italicized). Errors for all other values are expressed as the larger of either the 2SE of repeat analyses of an individual sample or the 2SD of repeat measurements of synthetic (NIST-3162a and SPEX) and natural rock standards (BCR-2) over the course of this study (i.e., external reproducibility).
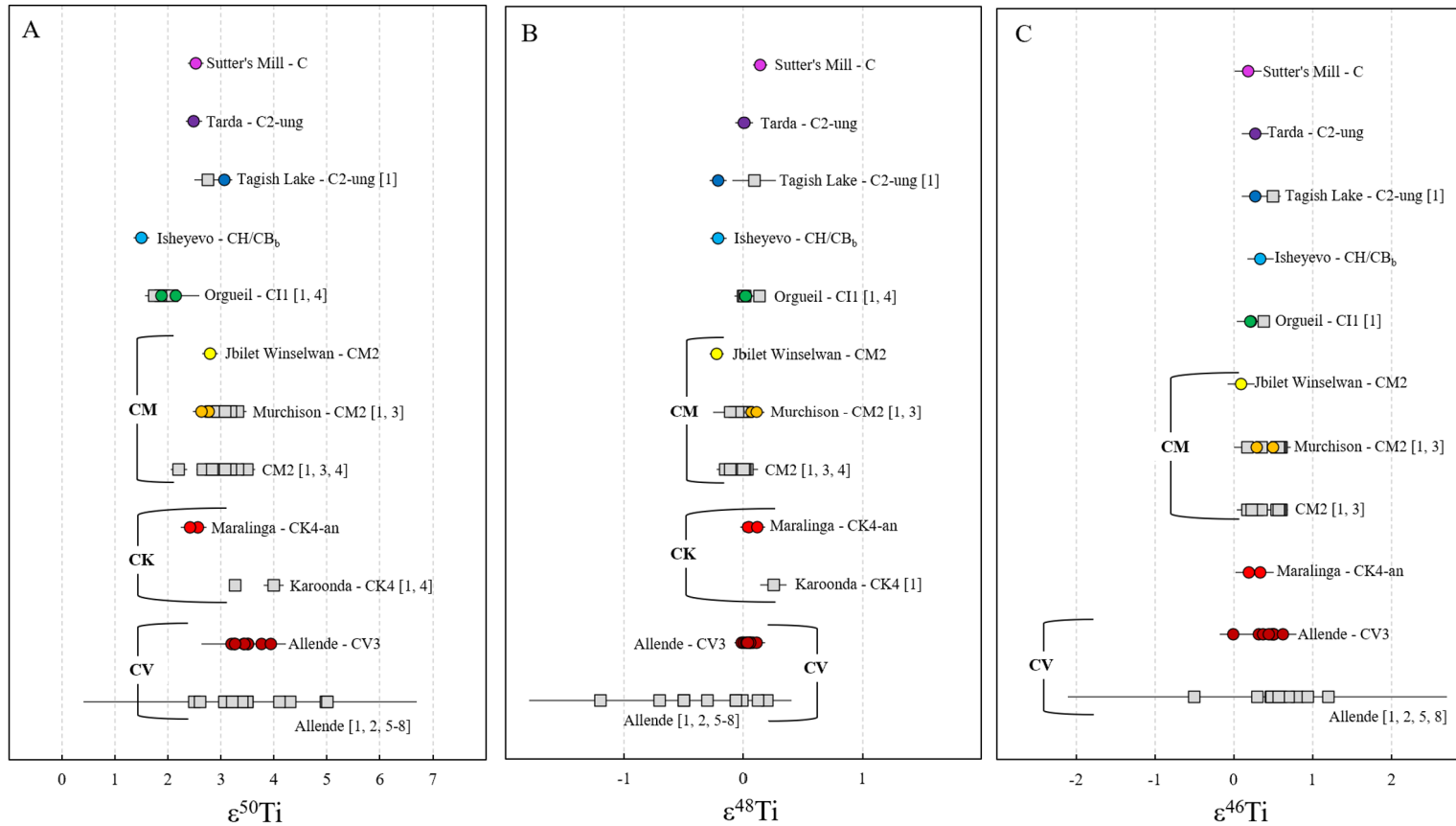
Figure 6. ε^{50}Ti (A), ε^{48}Ti (B), and ε^{46}Ti (C) values for the carbonaceous chondrite samples measured in this study. Literature values are gray circles, with the data source listed as a number next to the chondrite or group name. Measurements from this study are shown in color. The error on each data point from this study is the larger of either the 2SE of repeat analyses of an individual sample or the 2SD of repeat measurements of synthetic (NIST-3162a and SPEX) and natural rock standards (BCR-2) over the course of this study (n=45) (i.e., external reproducibility). Data sources: [1] Trinquier et al. (2009), [2] Torrano et al. (2019), [3] Torrano et al. (2021), [4] Zhang et al. (2012), [5] Leya et al. (2007), [6] Sandborn et al. (2019), [7] Williams et al. (2020), [8] Metzler et al. (2021).

5. DISCUSSION

5.1. Isotopic Variations and Sample Heterogeneity

As mentioned earlier, chondrites are comprised of various components with a wide range in the sizes of their nucleosynthetic anomalies. The heterogeneous distribution of these components in bulk samples (particularly at smaller sampling scales) likely results in variations in the reported data on the nucleosynthetic anomalies in these samples from one study to another. In this work, the use of relatively large sample fragments (~200 mg) minimized this effect. However, some previous studies of Ti isotope compositions have utilized relatively small sample sizes where isotopic heterogeneity at the sampling scale could become a more prominent factor. For example, Ti isotope values have now been reported for the Murchison (CM2) chondrite in three separate studies: Trinquier et al. (2009) (10 mg to 100 mg); Torrano et al. (2021) (~350 mg); and this study (~200 mg). As can be seen in Figure 7, the larger bulk fragments used in the two more recent studies seem to produce consistently lower ε^{50}Ti values. A likely explanation for the difference in the average ε^{50}Ti values based on the smaller samples of Trinquier et al. (2009) versus the larger samples of Torrano et al. (2021) and this study could be that the smaller samples contain a proportionally larger and non-representative fraction of components with higher ε^{50}Ti values (such as CAIs). However, further investigations will be required to ascertain this.
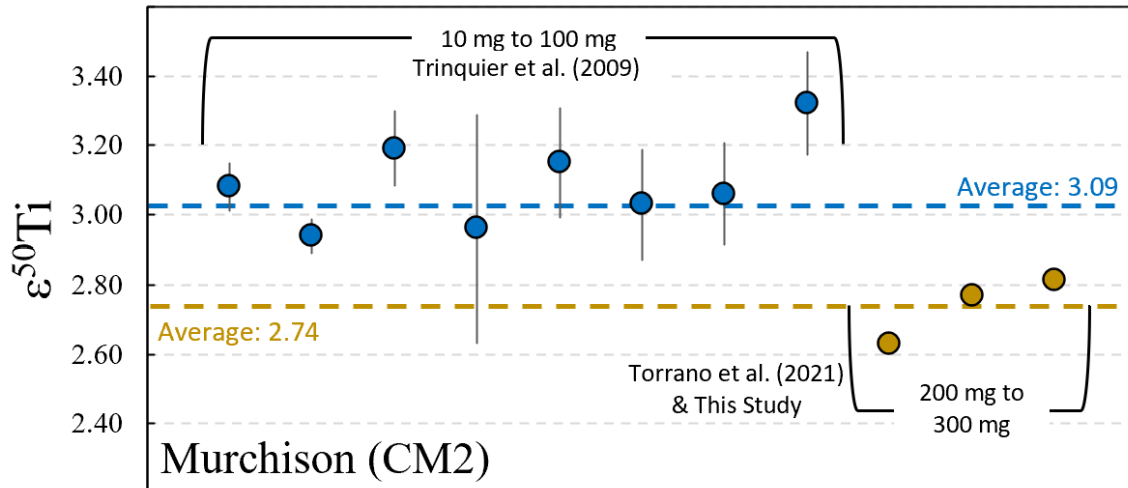
Figure 7. ε^{50}Ti values from three studies for the Murchison (CM2) chondrite. Blue circles represent values from Trinquier et al. (2009) determined on bulk samples ranging from 10 to 100 mg; the average ε^{50}Ti value for Murchison from that study is shown as the blue dashed line. Yellow circles represent values from Torrano et al. (2021) and this present study, where larger bulk samples (200-300 mg) were used; the average ε^{50}Ti value from these two studies is shown as the yellow dashed line. The error on each data point from this study is the larger of either the 2SE of repeat analyses of an individual sample or the 2SD of repeat measurements of synthetic (NIST-3162a and SPEX) and natural rock standards (BCR-2) over the course of this study (n=45) (i.e., external reproducibility).

5.2. Origin and Carrier(s) of Ti Isotope Anomalies

Several potential carriers of the anomalous Ti isotope signature are reported in CC materials. Calcium-Aluminum inclusions (CAIs) and presolar grains are the two commonly proposed candidates contributing to the anomalous signatures in bulk CC samples (e.g., Trinquier et al., 2009; Torrano et al., 2019; Nittler et al., 2018). The average ε^{50}Ti value of a CC group appears to increase with an increasing abundance of CAIs (Figure 8). The Maralinga sample used in this study reportedly has more CAIs than other CK samples (Keller et al., 1992). However, the ε^{50}Ti value reported here would suggest a lower CAI content or a heterogenous distribution of CAIs or presolar grains in the Maralinga matrix. Therefore, CAIs within the Maralinga sample should be measured

26

for Ti isotope compositions to test if the values match other CAIs. It is important to note that while there somewhat appears to be a correlation in Figure 8 between CAI abundance and averaged ε^{50}Ti values, this relation may not be valid for every sample Ti isotope composition measured. Heterogeneity in the distribution of presolar grains may also have affected the bulk Ti isotope compositions of these samples; more work is needed, possibly on presolar silicate grains, to determine how these materials contributed to the Ti isotope variations of these meteorites.
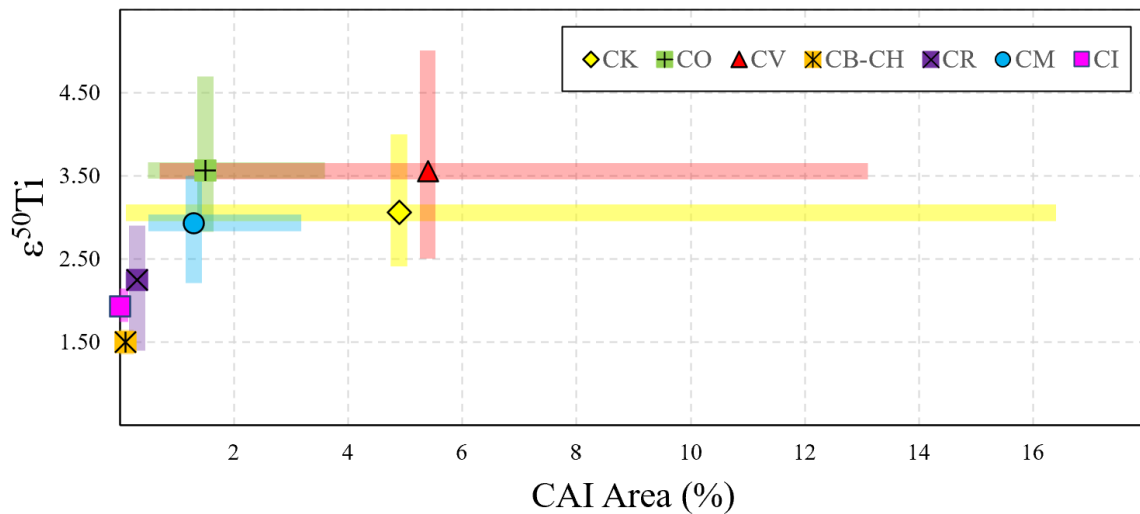
Figure 8. CAI area in percent (%) vs. ε^{50}Ti values for different CC groups. The horizontal and vertical colored bars represent the range of measurements determined by the minimum and maximum values measured for the CAI area (x-axis) and ε^{50}Ti values (y-axis) for each CC group. The data points represent the average value for each CC group's CAI area (%) and ε^{50}Ti value. CAI average area values are from Dunham et al. 2023. ε^{50}Ti values are from this study and previous work (Leya et al., 2007; Trinquier et al., 2009; Zhang et al., 2012; Williams et al., 2020; Torrano et al., 2019; Torrano et al., 2021; Sanborn et al., 2019 and Metzler et al., 2021).

The averaged ε^{50}Ti and ε^{46}Ti values for each CC group, with the new data added from this study, are shown in Figure 9. The averaged ε^{50}Ti and ε^{46}Ti values plot along the CAI correlation line from Torrano et al., 2023 (slope: 5.63 ± 0.29; intercept 0.19 ± 0.45). This

would suggest that CAIs do contribute to bulk CC Ti isotope values. However, Torrano et al. (2023) demonstrated that the Ti isotope values measured in CAIs might record mixing between early-formed refractory materials such as platy hibonite crystals (PLACs) and spinel-hibonite inclusions (SHIBs). As PLACs and SHIBs are often comprised of more anomalous Ti isotope compositions, it was argued that an averaging effect diluted the anomalous Ti isotope signatures in larger-sized chondritic materials like CAIs (Torrano et al., 2023).

The CAI and bulk CC correlation between ε^{50}Ti and ε^{46}Ti (Figure 9) could suggest two unique isotopic reservoirs in the early Solar System from which these materials formed. The nucleosynthesis of ^{46}Ti and ^{50}Ti are distinct in that the ^{46}Ti isotope is likely produced during explosive oxygen- and silicon burning in the outer region of the Si/S zone in Type II supernovae (SNII), whereas ^{50}Ti has been suggested to originate during Type Ia supernovae (SNIa), electron-capture supernovae (ECSN), and within the O/Ne and O/C regions of SNII (Torrano et al., 2023 and references therein). Although both isotopes can be produced in SNII, the multiple potential sources of ^{50}Ti, along with other isotope systems not discussed here, suggest a variety of unique isotope reservoirs.
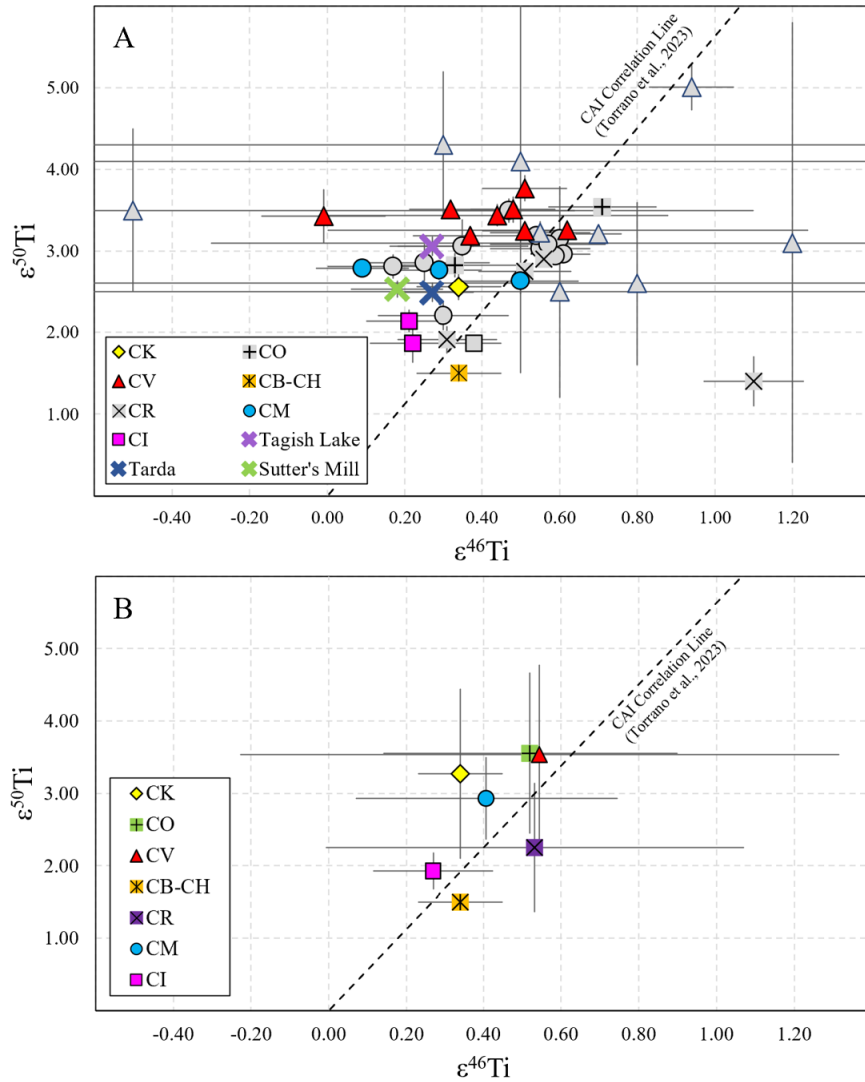
Figure 9. A. ε^{50}Ti vs. ε^{46}Ti values for different CC samples. Samples from this study are in color, while samples from the literature are in grey. B. Averaged ε^{50}Ti vs. averaged ε^{46}Ti values for different CC groups. The CAI Correlation Line was adopted from Torrano et al., 2023. The ε^{50}Ti and ε^{46}Ti group values are averaged from measurements in this study and previous work (Leya et al., 2007; Trinquier et al., 2009; Zhang et al., 2012; Williams et al., 2020; Torrano et al., 2019; Torrano et al., 2021; Sanborn et al., 2019 and Metzler et al., 2021). Errors for samples from this study are the larger of either the 2SE of repeat analyses of an individual sample or the 2SD of repeat measurements of synthetic (NIST-3162a and SPEX) and natural rock standards (BCR-2) over the course of this study (n=45) (i.e., external reproducibility). Errors in Subfigure B represent the calculated 2SD from the values used to calculate the group average.

5.3. Effect of Parent Body Accretion Timing on Anomalous Ti Isotope Signatures

As they relate to the NC and CC dichotomy, the differences in the Ti isotope compositions are not considered to be the result of differences in the timing of accretion of the NC and CC parent bodies (Bermingham et al., 2020). Furthermore, the inability to resolve differences in accretion ages between NC and CC materials makes it challenging to draw definite conclusions (Hilton et al., 2019). However, it is possible that within CC groups themselves, considering timing could provide some new insights. While there is evidence of multiple carriers for Ti isotope anomalies (e.g., PLACs, SHIBs; see section 5.2) CAIs are, at present, one of the most widely studied Ti isotope carriers (e.g., Torrano et al., 2019; Torrano et al., 2023) and thus potentially provide information about Ti isotopes in bulk sample CC materials. CAIs, a carrier of the ^{50}Ti isotope anomaly, are considered to have formed close to the Sun and were transported outwards (Bermingham et al., 2020). While the timing of this outward transport is not precisely known, if the availability of CAIs as accretionary material for forming parent bodies decreased over time, this could be shown in correlating the ^{50}Ti isotope compositions, proposed parent body accretion times and, even CAI abundance (see section 5.2). CC group accretion times are compared to averaged ε^{50}Ti values to see if a correlation exists between the two (Figure 9). The accretion times were used from the Sugiura & Fujiya (2014) study. The initial ^{26}Al/^{27}Al values used in Sugiura & Fujiya (2014) were determined based on the estimated maximum temperature for a CC group's parent body's interior. These accretion ages are within the error of other studies (Desh et al., 2011 and references therein). While there is a general downward trend in ε^{50}Ti values for samples accreted later, the

significant age errors and range of ^{50}Ti isotope compositions prevent a correlation between the two from being determined. Instead, this relation, or lack thereof, implies that other aspects, besides timing, of the parent body accretion affect ε^{50}Ti values (see section 5.2). One critical sample to note here is the Isheyevo (CH/CB$_b$); the ε^{50}Ti value for the CB-CH group is based on one bulk measurement from this study on Isheyevo. Therefore, more bulk measurements on Ti isotopes should be required for CH and CB samples to better constrain the variability of ε^{50}Ti measurements in that group.
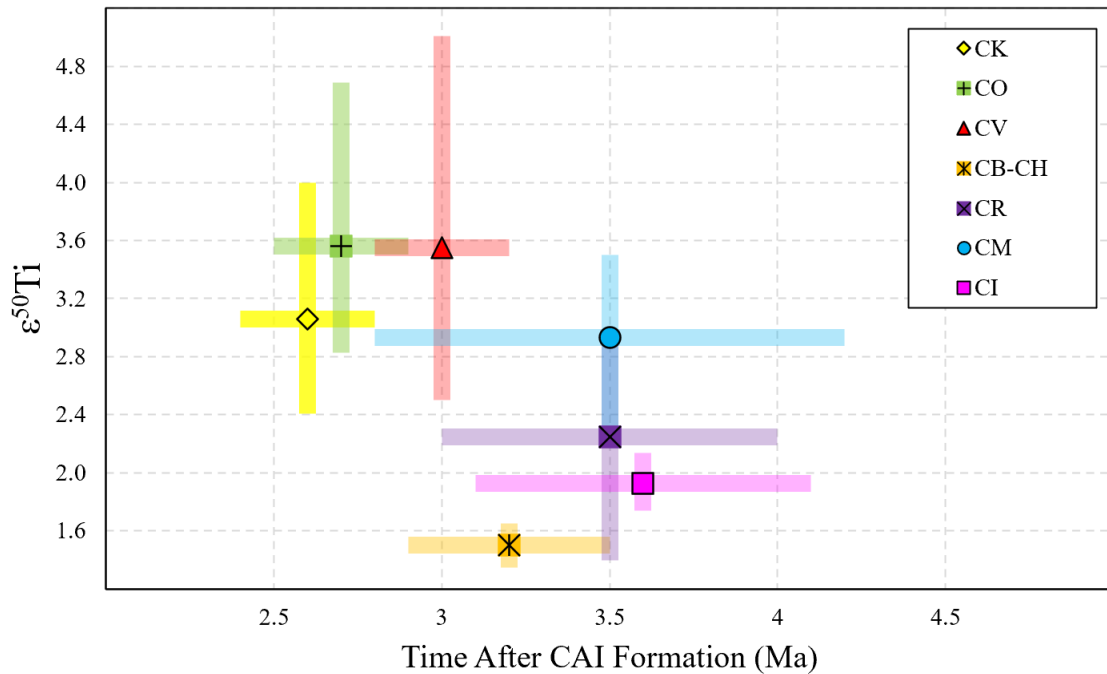
Figure 10. Parent body accretion times (after CAI formation) vs. ε^{50}Ti values for different CC groups. The data and colored horizontal bars for the accretion times represent the reported CC group accretion age (relative to CAI formation) and associated error from Sugiura & Fujiya (2014). The ε^{50}Ti data are average values for the CC groups calculated using measurements from this study and previous work (Leya et al., 2007; Trinquier et al., 2009; Zhang et al., 2012; Williams et al., 2020; Torrano et al., 2019; Torrano et al., 2021; Sanborn et al., 2019 and Metzler et al., 2021); the colored vertical bars associated with the ε^{50}Ti values represent the minimum and maximum values reported in the literature.

6. CONCLUSIONS

Results from this work expanded the range of bulk sample Ti isotope compositions for multiple CC groups. The majority of ε^{46}Ti values obtained in this study, excluding one Allende measurement, are positive relative to the terrestrial standards (Figure 6). The ε^{48}Ti values for the samples studied here show minor variations among these samples (Figure 6). The ε^{50}Ti values for CM2 chondrites are similar to those for the ungrouped carbonaceous chondrites (Figure 6). This similarity could suggest that these samples were sourced from a similar isotopic reservoir. The ε^{50}Ti values of the CI1 and CH/CBb bulk samples are lower than those of the other CC groups, suggesting that these samples may be sourced from reservoir(s) distinct from that of the other CC groups.

This work emphasizes the importance of representative sampling of chondritic meteorites for Ti isotopic analyses to infer the degree of isotopic heterogeneity in the solar nebula; this is well illustrated by the analyses of Murchison and Allende reported in this and previous studies. Future studies should take care to ensure representative sample sizes are used. Further investigations of the Ti isotopic compositions of such representative bulk samples, particularly for the CK, CH, and CB groups, will aid in better determining the extent of variation within those groups and thereby better constraining the degree of isotopic heterogeneity in the solar nebula.

There are likely multiple carriers for the anomalous Ti isotope signatures in bulk samples of CC meteorites. While CAIs and presolar grains are the two potential carriers discussed in this work, it is essential to note that other components like SHIBs and PLACs have recently been argued to contribute to the observed variations (Torrano et al.,

2023). With this being said, the correlation between ε^{50}Ti and ε^{46}Ti (which is also observed for CAIs) is still present when adding data from this study to the averaged values for the various CC groups (Figure 9), suggesting the two may be related to one another. Given the distinct nucleosynthetic sources proposed for these two isotopes, the correlation between ε^{50}Ti and ε^{46}Ti may indicate that the proportion of the distinct presolar grains that served as the carriers of each of these anomalous isotope signatures was relatively uniform in the solar nebula. While the abundance of CAIs and the accretion time appear to have some relationship to the ε^{50}Ti values, other factors may also play a role in the variations seen between groups (e.g., presolar grains, accretion distance from Sun, etc.).

REFERENCES

Amari S., Hoppe P., Zinner E., and Lewis R.S. (1992) Interstellar SiC with unusual isotopic compositions – Grains from a supernova? *Astrophysical Journal Letters*, **394**:L43-L46.

Arnold G.L., Weyer S. and Anbar A.D. (2004) Fe isotope variation in natural materials measured using high mass resolution multiple collector ICPMS. *Analytical Chemistry*, **76**, 322–327.

Barrat J.A., Zanda B., Moynier F., Bollinger C., Liorzou C., and Bayon G. (2012) Geochemistry of CI chondrites: Major and trace elements, and Cu and Zn Isotopes. *Geochimica et Cosmochimica Acta*, **83**, 79-92.

Bermingham K.R., Füri E., Lodders K. and Marty B. (2020) The NC-CC Isotope Dichotomy: Implications for the Chemical and Isotopic Evolution of the Early Solar System. *Space Science Reviews,* **216**, 133.

Bernatowicz T., Fraundorf G., Ming T., Anders E., Wopenka B., Zinner E and Fraundork P. (1987) Evidence for interstellar SiC in the Murray carbonaceous meteorite. *Nature*, **330**, 728–730.

Birck J-L, Allègre CJ (1984) Chromium isotopic anomalies in Allende refractory inclusions. *Geophysics Research Letters,* **11**, 943−946.

Bonal L., Huss G.R., Krot A.N., Nagashima K., Ishii H.A. and Bradley J.P. (2010) Highly ^{15}N-enriched chondritic clasts in the CB/CH-like meteorite Isheyevo. *Geochimica et Cosmochimica Acta*, **74**, 6590-6609.

Braukmüller N., Wombacher F., Hezel D.C., Escoube R., and Münker C. (2018) The chemical composition of carbonaceous chondrites: Implications for volatile element depletion, complementarity, and alteration. *Geochimica et Cosmochimica Acta*, **239**, 17–48.

Brown P.G., Hildebrand A.R., Zolensky M.E., Grady M., Clayton R.N., Mayeda T.K., Tagliaferri E., Spalding R., MacRae N.D., Hoffman E.L., Mittlefehldt D.W., Wacker J.F., Bird J.A., Campbell M.D., Carpenter R., Gingerich H., Glatiotis M., Greiner E., Mazur M.J., McCausland P.J., Plotkin H. and Rubak Mazur T. (2000) The fall, recovery, orbit, and composition of the Tagish Lake meteorite: a new type of carbonaceous chondrite. *Science*, **290** No. 5490.

Clayton D.D. (1982) Cosmic Chemical Memory: a New Astronomy. *Quarterly Journal of the Royal Astronomical Societ*y **23**, 174–212.

Clayton D.D. (2003) Handbook of Isotopes in the Cosmos: Hydrogen to Gallium. Cambridge, *Cambridge University Press,* 2003.

Dauphas N., Remusat L., Chen J. H., Roskosz M., Papanastassiou D. A., Stodolna J., Guan Y., Ma C. and Eiler J. M. (2010) Neutron-Rich Chromium Isotope Anomalies in Supernova Nanoparticles. *Astrophysical Journal,* **720**, 1577–1591.

Dauphas N. and Schauble E. A. (2016) Mass Fractionation Laws, Mass-Independent Effects, and Isotopic Anomalies. *Annual Review: Earth & Planetary Science,* **44**, 709–83.

Davidson J., Busemann H., Nittler L.R., Alexander C. M.O'D., Orthous-Daunay F.-R., Franchi I.A., and Hoppe P. (2014) Abundances of presolar silicon carbide grains in primitive meteorites determined by NanoSIMS. *Geochimica et Cosmochimica Acta,* **139**, 248–266.

Davis A.M., Zhang J., Greber N.D., Hu J., Tissot F.L.H., Dauphas N. (2018) Titanium isotopes and rare earth patterns in CAIs: Evidence for thermal processing and gas-dust decoupling in the protoplanetary disk. *Geochimica et Cosmochimica Acta,* **221**, 275–295.

Desch S.J., Kalyaan A., and Alexander C. M.O'D. (2011) The Effect of Jupiter's Formation on the Distribution of Refractory Elements and Inclusions in Meteorites. *The Astrophysical Journal Supplement Series,* **238**:11.

Dunham E.T., Sheikh A., Opara D., Matsuda N., Liu M-C., McKeegan K.D. (2023) Calcium Aluminum-rich inclusions in non-carbonaceous chondrites: abundances, sizes, and mineralogy. *Meteoritics and Planetary Science*, **58**, 643–671.

Hilton C.D., Bermingham K.R., Walker R.J., and McCoy T.J. (2019) Genetics, crystallization sequence, and age of the South Byron Trio iron meteorites: new insights to carbonaceous chondrite (CC) type parent bodies. *Geochimica et Cosmochimica Acta,* **251**, 217–228.

Hoppe P. and Ott U. (1997) Mainstream silicon carbide grains from meteorites. In: Bernatowicz TJ and Zinner E (eds.) *Astrophysical Implications of the Laboratory Study of Presolar Materials*, pp. 27–58. New York: AIP.

Hoppe P., Strebel R., Eberhardt P., Amari S., and Lewis R.S. (2000) Isotopic properties of silicon carbide X grains from the Murchison meteorite in the size range 0.5–1.5 mm. *Meteoritics & Planetary Science* **35**, 1157–1176.

Hoppe P, Fujiya W, and Zinner E (2012) Sulfur molecule chemistry in supernova ejecta recorded by silicon carbide stardust. *The Astrophysical Journal* **745**, L26–L30.

Huss G.R., Meshik A.P., Smith J.B., and Hohenberg C.M. (2003) Presolar diamond, silicon carbide, and graphite in carbonaceous chondrites: implications for thermal processing in the solar nebula. *Geochimica et Cosmochimica Acta,* **67**, 4823–4848.

Hynes K. M. and Gyngard F. (2009) The presolar grain database: http://presolar.wustl.edu/~pgd. *Lunar & Planetary Science Conference,* **40**, Abstract #1198.

Ivanova M.A., Kononkova N.N., Krot A.N., Greenwood R.C., Franchi I.A., Verchovsky A.B., Trieloff M., Korochantseva E.V. and Brandstätter F. (2008) The Isheyevo meteorite: Mineralogy, petrology, bulk chemistry, oxygen, nitrogen, carbon isotopic compositions, and ^{40}Ar-^{39}Ar ages. *Meteoritics & Planetary Science* **43**, 915–940.

Kallemeyn G. W. and Wasson J. T. (1981) The compositional classification of chondrites – I. The carbonaceous groups. *Geochimica et Cosmochimica Acta,* **45**, 1217–1230.
Keller L.P., Clark J.C., and Moore C.B. (1992) Maralinga, a metamorphosed carbonaceous chondrite found in Australia. *Meteoritics (ISSN 0026-1114)*, **27**, 87–91.

Kruijer T.S., Burkhardt C, Budde G., and Kleine T. (2017) Age of Jupiter inferred from the distinct genetics and formation times of meteorites. *Proceedings of the National Academy of Sciences*, **114**, 6712–6716.

Kurat G., Zinner E. and Brandstätter F. (2002) A plagioclase-olivine-spinel-magnetite inclusion from Maralinga (CK): evidence for sequential condensation and solid-gas exchange. *Geochimica et Cosmochimica Acta*, **66**, 2959–2979.

Krot A.N., Keil K., Scott E.R.D., Goodrich C.A., Weisberg M.K. (2014) Meteorites and Cosmochemical Processes – Classification of Meteorites and Their Genetic Relationships (1.0), Volume 1 of Treatise on Geochemistry (Second Edition). *Elsevier*, 2014. Edited by Andrew M. Davis, p.1-63

Lambert D.L., Gustafsson B., Eriksson K., and Hinkle K.H. (1986) The chemical composition of carbon stars. I. Carbon, nitrogen, and oxygen in 30 cool carbon stars in the galactic disk. *The Astrophysical Journal Supplement Series* **62**, 373–425.

Larsen K.K., Wielandt D., Schiller M. and Bizzarro M. (2016) Chromatographic speciation of Cr (III)-species, inter-species equilibrium isotope fractionation and improved chemical purification strategies for high-precision isotope analysis. *Journal of Chromatography A*, **1443**, pp. 162–174.

Lauretta D. S., Bartels A. E., Barucci M. A., Bierhaus E. B., Binzel R. P., Bottke W. F., CampinsH., Chesley S. R., Clark B. C., Clark B. E., Cloutis E. A., Connolly H. C., Crombie M. K., Delbó M., Dworkin J. P., Emery J. P., Glavin D. P., Hamilton V. E., Hergenrother C. W., Johnson C. L., Keller L. P., Michel P., Nolan M. C., Sandford S. A., Scheeres D. J., Simon A. A., Sutter B. M., Vokrouhlický D. and Walsh K. J. (2015) The OSIRIS-REx target asteroid (101955) Bennu: Constraints on its physical, geological, and dynamical nature from astronomical observations. *Meteoritics & Planetary Science,* **50**, 834–849.

Lauretta D. S., Al Asad M. M, Ballouz R.-L., Barnouin O. S., Bierhaus E. B., Boynton W. V., Breitenfeld L. B., Calaway M. J., Chojnacki M., Christensen P. R., Clark B. E., Connolly Jr., H. C., Drouet d'Aubigny C., Daly M. G., Daly R. T., Delbó M., Della Giustina D. N., Dworkin J. P., Emery J.P., Enos H. L., Farnocchia D., Golish D. R., Haberle C. W., Hamilton V. E., Hergenrother C. W., Jawin E. R., Kaplan H. H., Le Corre L., McCoy T. J., McMahon J. W., Michel P., Molaro J. L., Nolan M. C., Pajola M., Palmer E., Perry M. E., Reuter D. C., Rizk B., Roberts J. H., Ryan A., Scheeres D. J., Schwartz S. R., Simon A. A., Susorney H. C. M., Walsh K. J., Zou, X.-D. (2019) OSIRIS-REx arrives at asteroid (101955) Bennu: Exploration of a hydrated primitive near-Earth asteroid. *Lunar and Planetary Science Conference*, **50**. #2608.

Leya I., Schönbächler M., and Wiechert U. (2008) Titanium isotopes and the radial heterogeneity of the Solar System. *Earth & Planetary Science Letters,* **266**, 233–244.

Liu N., Nittler L.R., Pignatari M., Alexander C M. O'D., and Wang J. (2017) Stellar Origin of ^{15}N-rich Presolar SiC Grains of Type AB: Supernovae with Explosive Hydrogen Burning. *The Astrophysical Journal Letters*, **842**:L1.

Marrocchi Y., Avice G. and Barrat J-A. (2021) The Tarda Meteorite: A Window into the Formation of D-typeAsteroids. *The Astrophysical Journal Letters*, **913**:L9.

Metzler K., Hezel D., Barosch J., Wölfer E., Schneider J., Hellmann J., Berndt J., Stracke A., Gattacceca J., Greenwood R., Franchi I.A., Burkhardt C., and Kleine T. (2021) The Loongana (CL) group of carbonaceous chondrites. *Geochimica et Cosmochimica Acta*, **304**, pp.1-31.

Nguyen A.N., Nittler L.R., Alexander M.O'D. C. and Hoppe P. (2018) Titanium isotopic compositions of rare presolar SiC grain types from the Murchison meteorite. *Geochimica et Cosmochimica Acta,* **221**, 162–181.

Niederer F.R., Papanastassiou D.A., and Wasserburg G.J. (1981) The isotopic composition of titanium in the Allende and Leoville meteorites. *Geochim. Cosmochim. Acta* **45**, 1017–1031.

Nittler L.R., Alexander C. M.O'D., Liu N., and Wang J. (2018) Extremely ^{54}Cr- and ^{50}Ti-rich Presolar Oxide Grains in a Primitive Meteorite: Formation in Rare Types of Supernovae and Implications for the Astrophysical Context of Solar System Birth. *The Astrophysical Journal*, **856**, L24-L30.

Papanastassiou D.A. (1986) Chromium isotopic anomalies in the Allende meteorite. *The Astrophysical Journal*, **308**, L27-L30.

Paton C., Hellstrom J., Paul B., Woodhead J., Hergt J. (2011) Iolite: Freeware for the visualization and processing of mass spectrometric data. *Journal of Analytical Atomic Spectrometry*, **26**, 2508–2518.

Phan V. T.H., Rebois R., Beck P., Quirico E., Bonal L. and Noguchi T. (2022) Nanoscale mineralogy and organic structure in Orguiel (CI) and EET 92042 (CR) carbonaceous chondrites studied with AFM-IR spectroscopy. *Meteoritics & Planetary Science*, **57**, 3–21.

Qin L. and Carlson R.W. (2016) Nucleosynthetic isotope anomalies and their cosmochemical significance. *Geochemical Journal*, **50**, 43–65.

Render J., Ebert S., Burkhardt C., Kleine T. and Brennecka G.A. (2019) Titanium isotopic evidence for a shared genetic heritage of refractory inclusions from different carbonaceous chondrites. *Geochimica et Cosmochimica Acta*, **254**, 40-53.

Reynolds J.H. and Turner G. (1964) Rare Gases in the Chondrite Renazzo. *Journal of Geophysical Research*, **69**, 3263–3281.

Russell S.S., Zolensky M., Righter K., Folco L., Jones R., Connolly H.C., Grady M.M., and Grossman J.N. (2005) The Meteoritical Bulletin, No. 89, 2005 September. *Meteoritics & Planetary Science* **40**, Supplement: A201–A263.

Ruzicka A., Grossman J.N., and Garvie L. (2014) The Meteoritical Bulletin, No. 100. *Meteoritics & Planetary Science – Supplementary Material*, **49**, E1-E101.

Sanborn M.E., Wimpenny J., Williams C.D., Yamakawa A., Amelin Y., Irving A.J., and Yin Q-Z. (2019) Carbonaceous achondrites Northwest Africa 6704/6693: Milestones for early Solar System chronology and genealogy. *Geochimica et Cosmochimica Acta*, **245**, 577-596.

Schneider J.M., Burkhardt C., Marrocchi Y., Brennecka G.A. and Kleine T. (2020) Early evolution of the solar accretion disk inferred from Cr-Ti-O isotopes in individual chondrules. *Earth & Planetary Science Letters*, **551**, 116585.

Shukolyukov A. and Lugmair G.W. (2006) Manganese-chromium isotope systematics of carbonaceous chondrites. *Earth and Planetary Science Letters*, **250**, 200–213.

Teng F-Z, Dauphas N. and Watkins J.M. (2017) Non-Traditional Stable Isotopes: Retrospective and Prospective. *Reviews in Mineral Geochemistry,* **82**, 1–26.

Timmes FX, Woosley SE, Hartmann DH, and Hoffman RD (1996) The production of ^{44}Ti and ^{60}Co in supernovae. *The Astrophysical Journal,* **464**, 332–341.

Tomeoka K. and Buseck P.R. (1988) Matrix mineralogy of the Orgueil CI carbonaceous chondrite. *Geochimica et Cosmochimica Acta*, **52**, 1627-1640.

Torrano Z.A., Brennecka G.A., Williams C.D., Romanielo S.J., Rai V. K., Hines R. R. and Wadhwa M. (2019) Titanium isotope signature of calcium-aluminum-rich inclusions from CV and CK chondrites: Implications for the early Solar System reservoirs and mixing. *Geochimica et Cosmochimica Acta*, **263**, 13–30.

Torrano Z.A., Schrader D.L., Davidson J., Greenwood R.C., Dunlap D.R., and Wadhwa M. (2021) The relationship between CM and CO chondrites: Insights from combined analyses of titanium, chromium, and oxygen isotopes in CM, CO, and ungrouped chondrites. *Geochimica et Cosmochimica Acta*, **301**, 70–90.

Torrano Z.A., Brennecka G.A., Mercer C.M., Romaniello S.J., Rai V.K., Hines R.R., and Wadhwa M. (2023) Titanium and chromium isotopic compositions of calcium-aluminum-rich inclusions: Implications for the sources of isotopic anomalies and the formation of distinct isotopic reservoirs in the early Solar System. *Geochimica et Cosmochimica Acta*, **348**, 309–322.

Trinquier A., Elliott T., Ulfbeck D., Coath C., Krot A.N., and Bizzarro M. (2009) Origin of Nucleosynthetic Isotope Heterogeneity in the Solar Protoplanetary Disk. *Science*, **324**, 374-376

Urey H.C. (1952) The Planets: Their Origin and Development, *Yale University Press, New Haven*, pp 245.

Van Kooten E. M.M.E., Cavalcante L.L., Nagashima K., Kasama T., Balogh Z.I., Peeters Z., Hsiao S. S-Y., Shang H., Lee D-C., Lee T. Krot A.N. and Bizzarro M. (2018) Isotope record of mineralogical changes in a spectrum of aqueously altered CM chondrites. *Geochimica et Cosmochimica Acta*, **237**, 79–102.

Warren P.H. (2011) Stable-isotope anomalies and the accretionary assemblage of the Earth and Mars: A subordinate role for carbonaceous chondrites. *Earth & Planetary Science Letters,* **311**, 93–100.

Weisberg M.K., McCoy T.J., and Krot A.N. (2006) Meteorites and the Early Solar System II ed D. S. Lauretta and H.Y. McSween Jr., Tucson, AZ: *Univ. Arizona Press,* 19.

Williams C. D., Sanborn M. E., Defouilloy C., Yin Q.-Z., Kita N. T., Ebel D. S., Yamakawa A. and Yamashita K. (2020) Chondrules reveal large-scale outward transport of inner Solar System materials in the protoplanetary disk. *Proceedings of the National Academy of Science,* **117** (38), 23426–23435.

Zhang J., Dauphas N., Davis A.M. and Pourmand A. (2011) A new method for MC-ICPMS measurement of titanium isotopic composition: Identification of correlated isotope anomalies in meteorites. *Journal of Analytical and Atomic Spectrometry*, **26**, 2197–2205.

Zhang J., Dauphas N., Davis A.M., Leya I. and Fedkin A. (2012) The proto-Earth as a significant source of lunar material. *Nature: Geoscience Letters*, **5**, 251–255.

Zhu K., Moynier F., Schiller M., Alexander C. M.O'D., Davidson J., Schrader D.L., Kooten E. and Bizzarro M. (2021) Chromium isotopic insight into the origin of chondrite parent bodies and the early terrestrial volatile depletion. *Geochimica et Cosmochimica Acta*, **301**, 158-186.

Zinner E. (2014) Meteorites and Cosmochemical Processes – Presolar Grains (1.4), Volume 1 of Treatise on Geochemistry (Second Edition). *Elsevier*, 2014. Edited by Andrew M. Davis, p.1-63

Zolensky M.E., Nakamura K., Gounelle M., Mikouchi T., Kasama T., Tachikawa O. and Tonui E. (2002) Mineralogy of Tagish Lake: An ungrouped type 2 carbonaceous chondrite. *Meteoritics & Planetary Science* **37**, 737–761.

Zolensky M., Mikouchi T., Fries M., Bodnar R., Jenniskens P., Yin Q.-Z., Hagiya K., Ohsumi K., Komatsu M., Colbert M., Hanna R., Maisano J., Ketcham R., Kebukawa Y., Nakamura T., Matsuoka M., Sasaki S., Tsuchiyama A., Gounelle M., Le L., Martinez J., Ross K. and Rahman Z. (2014) Mineralogy and petrography of C asteroid regolith: The Sutter's Mill CM meteorite. *Meteoritics & Planetary Science* **49**, 1997-2016.

Zolensky M.E., Mikouchi T., Hagiya K., Ohsumi K., Komatsu M., Chan Q., Le L., Kring D., Cato M., Fagan A., Gross J., Tanaka A., Takegawa D., Hoshikawa T., Yoshida T. and Sawa N. (2016) Unique view of C asteroid regolith from the Jbilet Winselwan CM chondrite. *47th Lunar & Planetary Science Conference*.